Developmental Cell
Article

Dendrite Reshaping of Adult *Drosophila* Sensory Neurons Requires Matrix Metalloproteinase-Mediated Modification of the Basement Membranes

Kei-ichiro Yasunaga,[1,2] Takahiro Kanamori,[1,2] Rei Morikawa,[1,2] Emiko Suzuki,[3] and Kazuo Emoto[1,2,4,*]
[1]Department of Cell Biology, Osaka Bioscience Institute, 6-2-4 Furuedai, Suita, Osaka 565-0874, Japan
[2]Neural Morphogenesis Laboratory
[3]Gene Network Laboratory
National Institute of Genetics, 1111 Yata, Mishima, Shizuoka 411-8540, Japan
[4]PRESTO, Japan Science and Technology Agency, Saitama 332-0012, Japan
*Correspondence: emoto@obi.or.jp
DOI 10.1016/j.devcel.2010.02.010

SUMMARY

In response to changes in the environment, dendrites from certain neurons change their shape, yet the mechanism remains largely unknown. Here we show that dendritic arbors of adult *Drosophila* sensory neurons are rapidly reshaped from a radial shape to a lattice-like shape within 24 hr after eclosion. This radial-to-lattice reshaping arises from rearrangement of the existing radial branches into the lattice-like pattern, rather than extensive dendrite pruning followed by regrowth of the lattice-shaped arbors over the period. We also find that the dendrite reshaping is completely blocked in mutants for the matrix metalloproteinase (Mmp) 2. Further genetic analysis indicates that Mmp2 promotes the dendrite reshaping through local degradation of the basement membrane upon which dendrites of the sensory neurons innervate. These findings suggest that regulated proteolytic alteration of the extracellular matrix microenvironment might be a fundamental mechanism to drive a large-scale change of dendritic structures during reorganization of neuronal circuits.

INTRODUCTION

Neuronal circuits in the brain are not static. In many systems, especially during critical periods of development, neurons exhibit a period of juvenile plasticity in which connectivity can be modified in response to sensory input or following specific experiences, thereby providing neurons with new response properties, tailored to the new environment. To achieve these changes in connectivity, certain neurons modify the shape of their dendritic arbors in response to various stimuli (Cline, 2001; Lohmann and Wong, 2005; Wong and Ghosh, 2002). For example, retina ganglion cells (RGCs) modify their dendritic arbors as they mature in a sensory-evoked, activity-dependent manner (Bodnarenko and Chalupa, 1993). Likewise, mitral and tufted cells in the olfactory bulb initially have multiple primary dendrites that contact adjacent glomeruli; however, they eventually lose all but one dendritic branch that remains in contact with a single glomerulus (Malun and Brunjes, 1996). Over time, many types of neurons exhibit a reduction in structural plasticity, with neurons progressively reducing branch dynamics and stabilizing their dendritic arbors. For example, in hippocampal pyramidal neurons, the proportion of stable dendritic spines increases over time (Holtmaat et al., 2005; Zuo et al., 2005). Even in the case of adult-born neurons that integrate into existing neural circuits, dendrites enter a maintenance phase after a short period of dynamic growth and dendrite arbor rearrangement (Mizrahi, 2007). However, dendritic arbors of mature neurons often undergo drastic reshaping under pathological conditions, such as epilepsy and after ischemia. (Spigelman et al., 1998; Ruan et al., 2006). Therefore, understanding the mechanisms that underlie the dendrite arbor reshaping has important implications for understanding normal development of dendrite arbors, regulation of structural plasticity of dendrites, and dendritic pathology.

Although the mechanisms responsible for regulating structural plasticity of mature dendrites remain elusive, reshaping of dendrite arbors appears to be controlled not only by intrinsic factors, but also by extrinsic mechanisms, including modification of the extracellular matrix (ECM) (Cline, 2001; Wong and Ghosh, 2002; Pavlov et al., 2004). The ECM exerts a strong influence on dendrite morphogenesis in cultured neurons, as ECM can affect dendrite patterning, in part through ECM-neurite adhesive contacts mediated by cell adhesion molecules, such as integrins (Reichardt and Tomaselli, 1991). ECM-neurite interactions have also been implicated in regulating structural plasticity of dendrites in vivo, since blockage of the integrin-ECM interaction in RGCs (Marrs et al., 2006) or genetic ablation of the integrin-mediated signaling in adult cortical neurons (Moresco et al., 2005) causes progressive retraction of dendritic branches. How broadly the ECM is involved in regulating remodeling of neuronal circuits is currently unknown, but recent studies demonstrate that the ECM undergoes dynamic changes in the developing brain, and that the ECM development is affected in pathological conditions (Pavlov et al., 2004; Yong, 2005), suggesting that the ECM modifications may accompany remodeling of neuronal circuits. Indeed, recent studies suggest that local

degradation of the ECM plays an important role in structural plasticity of dendritic spines in response to neuronal activity (Frischknecht et al., 2009; Magata et al., 2004; Oray et al., 2004). The ECM modifications in the nervous system are likely achieved by the concerted actions of several different proteases that are secreted by neurons and glial cells (Dzwonek et al., 2004; Page-McCaw et al., 2007; Yong, 2005). Among these many proteases, the members of the matrix metalloproteinase (MMP) family stand out as likely regulators of the dendrite development and pathology, because the MMPs are dramatically upregulated in particular neurons of the developing brain and in pathological conditions, and are often colocalized with dendrites. The MMPs stand out because they are dramatically upregulated in particular neurons of the developing brain and in pathological conditions, and are often colocalized with dendrites (Sekine-Aizawa et al., 2001; Szklarczyk et al., 2002). However, in large part due to issues of redundancy and compensation among over 20 vertebrate MMP family members, the in vivo role of MMPs in the nervous system remains to be established. In this regard, *Drosophila* affords an attractive genetic model system in which to study MMP functions, since there are only two MMP family members in the fly: Mmp1 and Mmp2 (Llano et al., 2000, 2002; Page-McCaw et al., 2003).

The *Drosophila* dendrite arborization (da) sensory neurons provide a suitable system for systematic analysis of dendritic morphogenesis (Gao et al., 1999; Jan and Jan, 2003; Parrish et al., 2007). Recent studies have demonstrated that the subtype-specific dendritic patterns of class IV da (C4 da) neurons are determined by intrinsic factors, such as transcription factors (Gao, 2007; Parrish et al., 2007), as well as extrinsic cues, such as repulsive interactions between neighboring dendrites (Emoto et al., 2004, 2006; Grueber et al., 2002; Koike-Kumagai et al., 2009). The C4 da neurons are born by mid-embryogenesis, and extend their two-dimensional dendrites between the epidermis and the underlying musculature during the late-embryonic and larval stages (Bodmer and Jan, 1987; Grueber et al., 2002). Following a period of growth and development in larval stages, the larval dendritic arbors are completely replaced with adult-specific processes as a result of extensive pruning and subsequent regeneration of dendrite arbors during metamorphosis (Kuo et al., 2005; Shimono et al., 2009; Williams and Truman, 2005). In contrast to the significant progress being made to understand embryonic/larval dendrite morphogenesis in C4 da neurons, much less is known about how C4 da neurons remodel and regenerate their dendritic arbors in the pupal/adult stages.

In this study, we investigated the arbor dynamics of C4 da neurons following elaboration of the adult-specific dendrite arbors, and found a rapid, highly stereotyped reshaping of these dendrite arbors following eclosion. Similar to their larval counterparts, dendrites of adult C4 da neurons initially elaborated dendritic trees in a radial fashion, and covered the whole body wall prior to eclosion. However, in contrast to what is observed during larval development, this radial arrangement of the dendritic arbor was rapidly rearranged to a lattice-like shape within 24 hr after eclosion. Time-lapse imaging revealed that this radial-to-lattice reshaping was largely due to rearrangement of the existing radial processes into a lattice-like pattern, rather than extensive pruning of the radially arranged dendrites followed by regrowth of new arbors into a lattice pattern. Mutations in *Mmp2*, which encodes a GPI-anchored MMP, blocked this radial-to-lattice reshaping of C4 da dendrites without affecting other aspects of dendrite growth or development, and Mmp2 expression in epithelial cells adjacent to C4 da dendrites was transiently increased at exactly the time when C4 da dendrites undergo the radial-to-lattice reshaping. Therefore, Mmp2 is a critical regulator of the dendrite arbor reshaping. Furthermore, we have found that epithelial Mmp2 promotes the dendrite reshaping through local modification of the basement membrane (BM) upon which C4 da dendrites grow, suggesting that alteration of the ECM microenvironment might be a general mechanism for driving the structural plasticity of dendritic arbors in vivo.

RESULTS

Dendrite Reshaping in Adult Sensory Neurons

During *Drosophila* metamorphosis, all three C4 da neurons degrade their larval dendrites by 15 hr after puparium formation (APF), and two of them, the dorsal ddaC neuron and the ventral-lateral v'ada neuron (Figure 1A), subsequently regenerate adult dendrites starting at ~50 hr APF while the ventral vdaB neuron undergoes apoptosis (Kuo et al., 2005; Williams and Truman, 2005). We focused on the v'ada neurons for our studies of the arbor dynamics during dendrite regrowth because the dorsal ddaC dendrites are difficult to image due to tanning of the cuticle as adults age. We monitored the morphological changes of the v'ada neurons throughout the regeneration process by using the C4 da neuron-specific *pickpocket* (*ppk*)-Gal4 driving mCD8GFP (Kuo et al., 2005). Consistent with prior reports (Kuo et al., 2005; Williams and Truman, 2005), dendritic processes of the larval C4 da neurons were completely removed by 15 hr APF, while the soma and axonal projections remained intact. Beginning at ~50 hr APF, these neurons began to extend fine protrusions, and by the time of pupal eclosion, these neurons elaborated dendritic arbors that cover the ventral-lateral body wall in a complete but nonredundant manner (Figures 1B and 1C). This tiling arrangement of C4 da dendrites, as well as the radial shape of individual dendrite arbors, is reminiscent of what has been observed in the larval C4 da neurons (Emoto et al., 2004, 2006; Grueber et al., 2002). To our surprise, however, the dendrite arbors of these adult C4 da neurons were dramatically rearranged within 24 hr after eclosion. Although no directional preference was detectable in C4 da dendrites at the time of eclosion (Figure 1C), many major dendrite branches, as well as the majority of terminal dendrite branches, became oriented along the dorsal-ventral (DV) axis by 24 hr after eclosion (Figure 1D). This lattice-like structure became more pronounced by 96 hr after eclosion (Figure 1E) and persisted throughout the adult stages (data not shown).

The radial-to-lattice reshaping of dendritic trees could result from pruning of the radially arranged dendrite branches followed by growth of the new lattice-shaped branches over the time interval, or from rearrangement of the existing radially oriented branches along the DV axis. To distinguish between these possibilities, we conducted time-lapse analysis of single adult neurons over a 72 hr time interval beginning at the time of eclosion (Figures 1F and 1G). All of the major branches and most of the

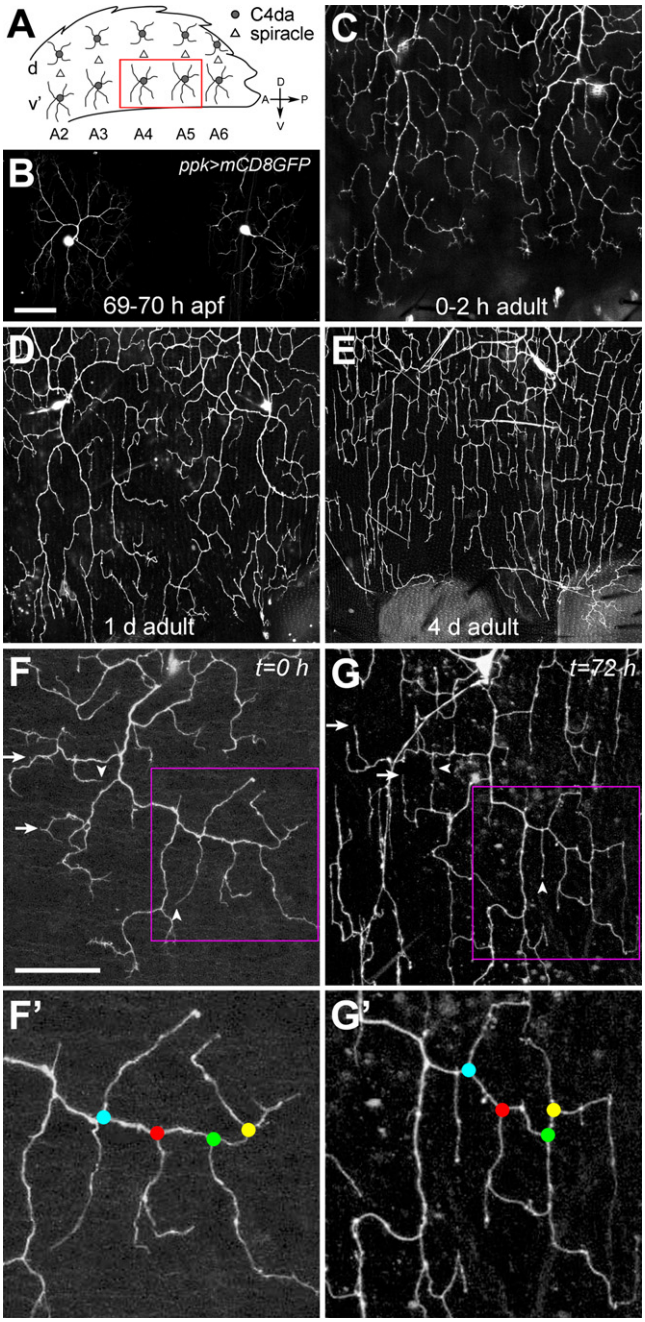

Figure 1. Dendrite Reshaping in Adult *Drosophila* Sensory Neurons

(A) Schematic representation of C4 da neurons in the adult ventral abdomen. The red box indicates the abdominal segments A4 and A5 in the lateral-ventral region that we analyzed in this study.

(B–E) Representative images of the lateral-ventral v'ada C4 da neurons in the late pupal (B) and the early adult stages (C–E).

(F–G) Dendritic pattern of a single C4 da neuron in 0 hr (F and F') and 72 hr (G and G') posteclosion adults. (F') and (G') show magnified images of the boxed region in (F) and (G), respectively. Corresponding branch points are marked by color-coded circles at the two time points. Arrows and arrowheads denote branches that elongated or retracted over the period, respectively. Scale bars, 50 μm.

dendrite branch points (70.2 ± 4.6%; n = 8) that were present at the time of eclosion persisted throughout the time lapse (Figures 1F' and 1G'). However, the radially oriented dendrite branches became dramatically rearranged along the DV axis over the time course. In contrast to the large-scale rearrangement that we observed in major branches, a small population of terminal branches showed growth (Figure 1G, arrows) or retraction (Figure 1F, arrow heads) over this period. These observations indicate that the radial-to-lattice reshaping of dendritic trees is predominantly achieved by rearrangement of the existing radial branches into a lattice-like pattern.

Dendrites Are Rearranged along the Lateral Tergosternal Muscle Fibers

Similar to the larval C4 da dendrites (Bodmer and Jan, 1987; Grueber et al., 2002), adult C4 da dendrites grow between the epidermis and the underlying musculature (lateral tergosternal muscles [LTMs]) (Figure 2G). Therefore, one possible mechanism for the dendrite reshaping is that surrounding tissues, such as the epidermis and/or the LTMs, may provide instructive cues to promote the radial-to-lattice reshaping of C4 da dendrites. To test this possibility, we first examined the positional relationship between dendrites and the epithelial cells or the LTM fibers during the rearrangement of C4 da dendritic arbors (Figures 2A–2F). At all time points of our analysis, we found no positional correlation between the dendritic branches and the epidermal intercellular boundaries (Figures 2A–2C). Similarly, dendrites and the LTMs did not show any positional correlation by 0–4 hr after eclosion (Figure 2D). Within 24 hr after eclosion, however, some major branches, as well as terminal branches, became aligned with the LTMs, and, eventually, the reshaped dendrites showed a striking correlation with the LTM fibers by 3 days after eclosion (Figures 2E and 2F). These observations suggest that C4 da dendrites are rearranged along the LTM fibers in the early adult stage.

Next, to simultaneously visualize the C4 da dendrites and the LTMs in the reshaping process, we developed a fly strain expressing the myosin heavy chain promoter-driven mCherry (MHC::mCherry) in combination with *ppk*Gal4 driving mCD8GFP in C4 da neurons (Figures 2H and 2I). This system allowed us to monitor the growth and the position of C4 da dendrites relative to the LTM fibers throughout the reshaping process. In our time-lapse imaging, we often observed major dendrite branches gradually moving toward the grooves between the LTM fibers (Figure 2H; see also Movie S1 available online). We also frequently observed the elongation of terminal branches along the LTMs (Figure 2I; Movie S2). Interestingly, nascent dendrite branches sprouted both inside and outside of the grooves between the LTMs; however, the latter ones immediately disappeared, suggesting that protrusions sprouting inside of the grooves are selectively maintained (Figure 2I, arrows). In addition, although terminal dendrites sometimes extended toward the outside of the LTM grooves, they immediately retracted and then restarted elongation inside the grooves (Figure 2I, arrow heads). These branch behaviors suggest that the terminal elongation is promoted by the microenvironment inside of the LTM grooves and/or inhibited by the microenvironment outside of the grooves.

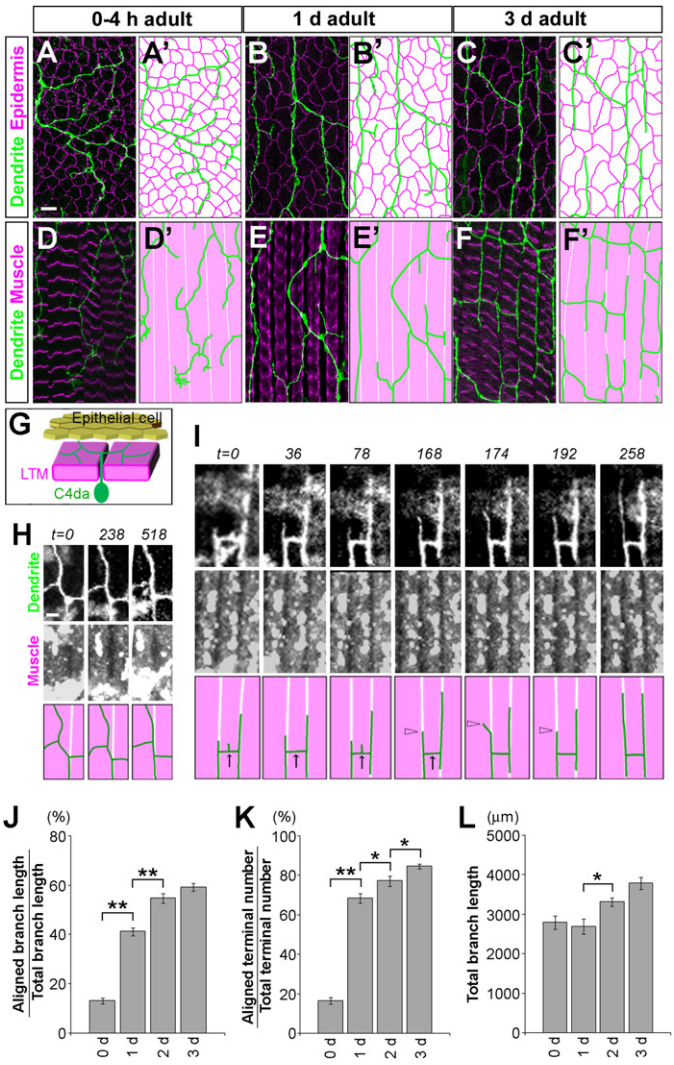

Figure 2. C4 da Dendrites Are Rearranged along the LTMs

(A–C) C4 da dendrites and the epidermal cell boundaries were visualized by anti-CD8 (green) and anti-armadillo antibody (magenta), respectively. Representative images and the corresponding traces were shown for 0–4 hr (A and A'), 1 day (B and B'), and 3 days (C and C') adults. Scale bars, 10 μm.

(D–F) C4 da dendrites and the LTM fibers were visualized by anti-CD8 (green) and rhodamin-phalloidin (magenta), respectively. Representative images and the corresponding traces were shown for 0–4 hr (D and D'), 1 day (E and E'), and 3 days (F and F') adults.

(G) Schematic representation depicting the spatial arrangement of epithelial cells (yellow), LTMs (magenta), and C4 da neurons (green) in the adult abdomen.

(H and I) Live imaging of C4 da dendrites during dendrite reshaping. Representative images showing lateral movement of the existing major branches (H) and elongation of terminal branches along the LTM fibers (I). C4 da dendrites (top panels), LTMs (middle panels), and the corresponding tracings (bottom panels) in the same fields are shown. Time scales indicate minutes. Scale bars, 5 μm.

(J–L) Quantification of the aligned branch length normalized to the total branch length (J), the aligned terminal number normalized to the total terminal number (K), and the total branch length (L) at four different time points during the early adult stages. Error bars indicate the mean ± SEM (Day 0, n = 11; Day 1, n = 8; Day 2, n = 7; Day 3, n = 18). *p < 0.05, **p < 0.01 (Student's t test).

Quantitative analysis indicated that, although less than 15% (13.2 ± 1.2%; n = 11) of the total number of dendritic branches was aligned to the LTMs by 5–7 hr after eclosion, ~40% (41.2 ± 1.6%; n = 8; p < 0.01) became aligned to the LTMs by 24 hr after eclosion (Figure 2J). The fraction of branches aligned with the LTMs gradually increased over the next 2 days (Figure 2J). A similar progression was observed in the number of the aligned dendritic terminals (Figure 2K). In contrast, although the total branch length was not changed significantly within 24 hr after eclosion, it was increased at a nearly constant rate over the next 2 days (Figure 2L). These results suggest that the dendrite reshaping is achieved by two distinct branch behaviors: rearrangement of the existing branches along the LTMs in the earlier stage, and elongation of the new terminal branches along the LTMs in the later stage.

Mmp2 Mutants Are Defective in Dendrite Reshaping

To gain insight into the molecular mechanism underlying the dendrite reshaping, we examined a collection of mutants that affect morphogenesis of the larval C4 da dendrites for effects on this radial-to-lattice dendrite reshaping (Table S1), and found that mutations in the *Mmp2* caused significant defects in the dendrite reshaping in the early adult stage (Figures 3A and 3B). Because *Mmp2* null mutants die as pupae, we monitored the effects of reducing Mmp2 function on this dendrite reshaping in viable adult escapers with the *trans*-heterozygous combination of a weak *Mmp2* allele and deficiency ($Mmp2^{F219I/Df}$) (Page-McCaw et al., 2003). Remarkably, dendritic arbors of C4 da neurons in these *Mmp2* mutant adults remained in the radial shape at 2 days after eclosion (Figure 3B), and these defects persisted at later adult stages (5~7 day adult: data not shown). Quantification of the LTM-aligned branch length revealed that only ~20% of the total dendritic branches in *Mmp2* neurons was aligned to the LTM fibers at the 2 day adult stage, compared with ~60% of the total branch length in wild-type dendrites (Figure 3C; wild-type, 56.8 ± 4.4%, n = 3; *Mmp2*, 18.7 ± 0.4%, n = 5; p < 0.05). Similar results were obtained in the number of aligned terminals (Figure 3D). In contrast, no significant difference was detected in the total dendrite branch length between wild-type controls and *Mmp2* mutants (Figure 3E), demonstrating that Mmp2 is required for the radial-to-lattice rearrangement, but is dispensable for branch growth of C4 da dendrites. Furthermore, the dendrite reshaping defects in *Mmp2* mutants are not due to a delay in the reshaping process or generalized dendrite growth defects.

To characterize the cellular basis of the *Mmp2* mutant phenotype, we next conducted time-lapse microscopy of single neurons. We focused our analysis on dendrite dynamics during the first 48 hr after eclosion, since our earlier analysis revealed that the majority of the dendrite reshaping occurs within this time frame. In both wild-type controls and *Mmp2* mutants, many of the terminal branches remained dynamic from the beginning (Figures 3F and 3I) to the end (Figures 3G and 3J) of the 48 hr period. Nearly 50% (wild-type, 47.3 ± 5.3%, n = 169;

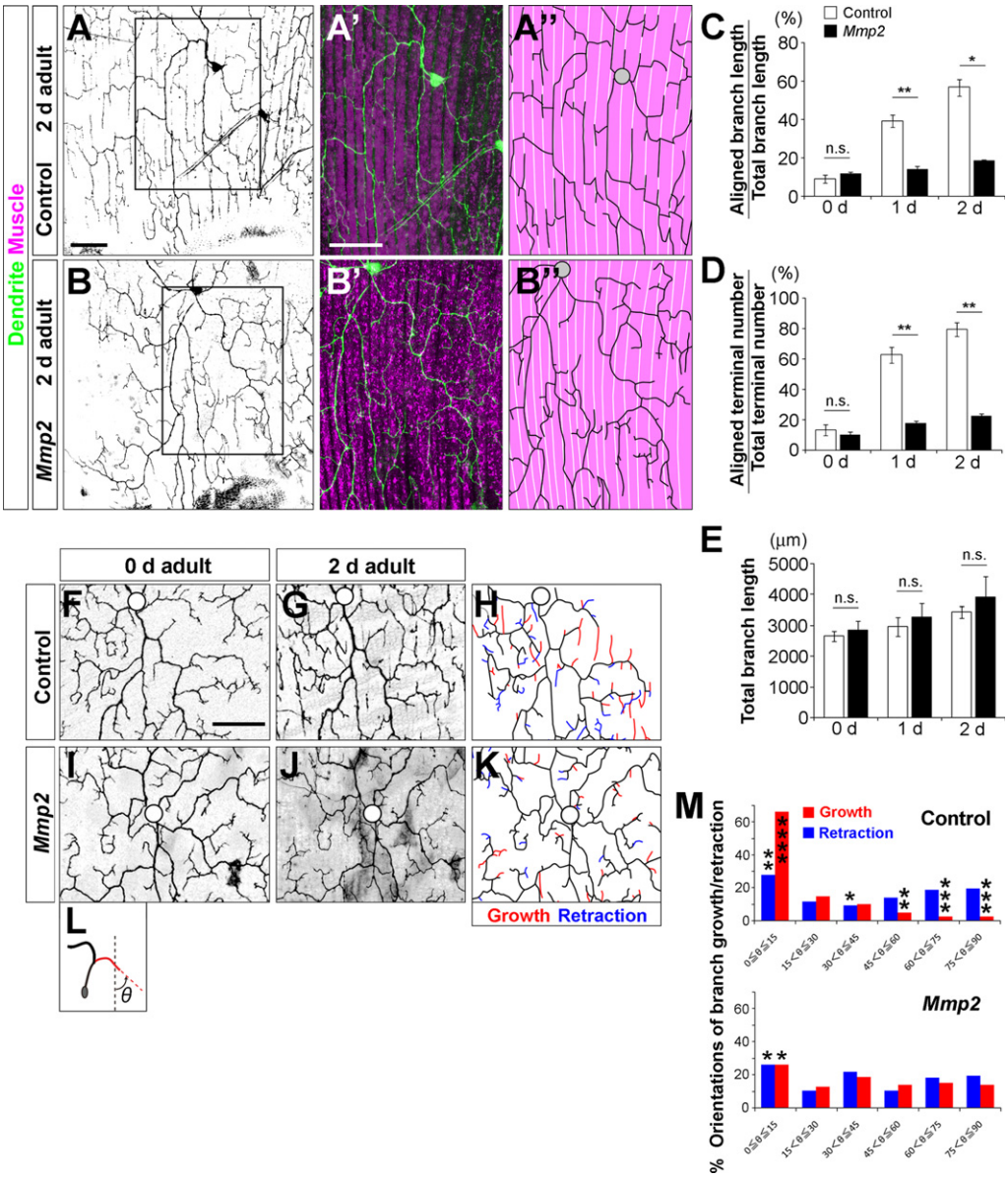

Figure 3. Mmp2 Is Required for Dendrite Reshaping in Adult *Drosophila* Sensory Neurons

(A and B) Morphology of C4 da dendrites of wild-type control (A–A") and *Mmp2* mutants (B–B") at 2 days posteclosion. Dendrites and LTMs were visualized by GFP (green) and MHC::mCherry (magenta), respectively. (A'–A") and (B'–B") are higher magnifications and the corresponding tracings of boxed regions in A and B, respectively. Genotypes: *ppkGal4*, *UAS-mCD8GFP* (A), and *ppkGal4, UAS-mCD8GFP; Mmp2^{F219I}/Mmp2^{Df}* (B).

(C–E) Quantification of the aligned branch length normalized to the total branch length (C), the aligned terminal number normalized to the total terminal number (D), and the total branch length (E) in wild-type control (white bars) and *Mmp2* mutants (black bars) in the early adult stages. Error bars indicate the mean ± SEM (wild-type control, n = 3; *Mmp2,* n = 6). *p < 0.05, **p < 0.01. n.s., not significant (p > 0.05) (Student's t test).

(F–L) Dendrites of the same neurons from 0 to 2 days posteclosion in wild-type controls (F and G) and *Mmp2* mutants (I and J). (H) and (K) are schematic views of wild-type controls and *Mmp2* mutants, respectively. Red and blue indicate net growth and net retraction, respectively. (L) We define θ as the angle of the dynamic branch terminals relative to the DV direction (dotted line). The DV direction was defined as the spiracle-to-sternite direction.

(M) Quantitative measurements of the orientations of dynamic branch terminals in wild-type control and *Mmp2* mutants. We performed binomial test by using the Pearson's Chi-square test. *p < 0.05, **p < 0.01, ***p < 0.001, ****p < 0.0001 (binomial test, wild-type control, n = 169; *Mmp2*, n = 168). Scale bars, 50 μm (A, B, and F–K).

Mmp2, 47.8 ± 1.5%, n = 168) of the dynamic branches displayed a net extension (Figures 3H and 3K, marked in red), whereas 50% (wild-type, 52.7 ± 5.3%, n = 169; *Mmp2*, 52.2 ± 1.5%, n = 168) showed a net retraction (Figures 3H and 3K, marked in blue) in both wild-type and *Mmp2* mutants. These observations indicate that dendrites in *Mmp2* mutants are not simply defective in branch dynamics. However, we observed a significant reduction in major dendrite branch rearrangements in

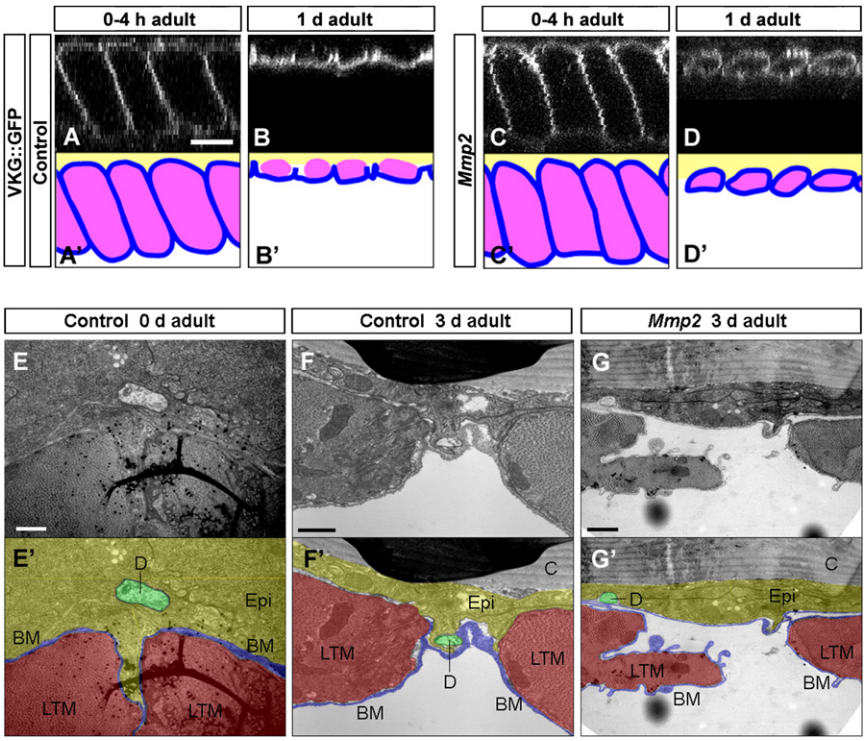

Figure 4. Mmp2 Is Required for BM Modification in the Adult Stage

(A–D) Confocal cross-sections of the BM, which are labeled with VKG::GFP at 0–4 hr (A and C) and 1 day adult (B and D). The BM at the interface between the epidermis and the LTMs is selectively degraded within 24 hr after eclosion in wild-type control (A and B). This BM modification is completely blocked in *Mmp2* mutants (C and D). (A'–D') Schematic representation of the tissues including epidermis (yellow), LTMs (magenta), and BM (blue). Scale bars, 10 μm.

(E–G) Electron micrograph of the abdominal body wall of a wild-type control animal at the 0–4 hr adult stage (E), a wild-type control animal at the 3 day adult stage (F), and an *Mmp2* mutant at the 3 day adult stage (G). (E'), (F'), and (G') are the colored images corresponding to (E), (F), and (G), respectively. Dendrites are marked in green, LTM fibers in magenta, BM in blue. A sagittal section of a 3 day adult provides the spatial relationship between epithelial cells (Epi), LTM fibers (LTM), C4 da dendrites (D), BM, and cuticle (C). Note that the dendritic branch is in contact with the epithelial cells and the BM, but not the LTMs in wild-type controls at the 3 day stage. Scale bars, 500 nm.

Mmp2 mutants over the period, demonstrating that Mmp2 function is required for these dendrite rearrangements. Finally, although ~65% of the growing branches became oriented along the DV axis in wild-type adults, growing dendrites in *Mmp2* mutants showed no obvious preference in the direction of growth (Figures 3L and 3M). Therefore, Mmp2 is required for both the rearrangement of major dendrite branches and the DV-directed growth of dendritic terminals along LTM fibers, but is dispensable for dendrite elongation/branching following eclosion.

Mmp2 Is Required for BM Modification in the Early Adult Stage

Given that Mmp2 plays a major role in modification of the BM by cleaving multiple ECM components (Srivastava et al., 2007; Uhlirova and Bohmann, 2006), we next monitored the BM dynamics by using a VKG::GFP protein trap line (GFP is fused with the collagen IV protein encoded by the *viking* gene) as a marker for the BM (Morin et al., 2001). The GFP signal was visible at the interface between the epidermis and the LTMs, as well as underneath the LTMs, by 0–4 hr after eclosion (Figure 4A). As reported previously (Kimura and Truman, 1990), the LTM fibers became significantly atrophied within 24 hr after eclosion (Figures 4A and 4B). Interestingly, during the same time period, the BM at the interface between the epidermis and the LTMs disappeared, whereas the BM along the LTM fibers, as well as underneath the LTMs, was maintained (Figure 4B). Remarkably, this local BM degradation was completely inhibited in *Mmp2* mutants, whereas the LTM atrophy appeared to proceed normally (Figures 4C and 4D).

Next, to monitor these cellular rearrangements with higher resolution, we performed electron microscopy (EM) studies of posteclosion flies. In cross sections taken perpendicular to the body wall of 0–4 hr (Figures 4E and 4E') and 3 day (Figures 4F and 4F') posteclosion adults, we found that the dendrites moved from the epidermal layer into the groove between the LTM fibers. Notably, dendritic branches in the groove did not appear to be closely associated with the LTMs, but rather were in direct apposition with the epithelial cells and the BM (Figures 4F and 4F'). We further analyzed the association of dendrites and the BM in serial EM sections of single branches, and found that the reshaped dendritic branches were closely juxtaposed to the BM at all places we observed, whereas less than 5% branches appeared to be associated with the LTMs (Figure S2), suggesting that a positive interaction may exist between the reshaped dendrites and the BM in the grooves. In *Mmp2* mutants, the movement of dendrites from the epidermis layer into the grooves was completely blocked, although the LTM fibers became atrophied to form grooves (Figures 4G and 4G''; Figure S2). Taken together, these data suggest that Mmp2 is required for the local modification of the BM at the interface between epidermis and LTMs during the first 24 hr after eclosion, and that the dynamic changes of the BM may play an active role in promoting dendrite reshaping.

Mmp2 Expression Is Transiently Upregulated in Epithelial Cells at the Time when C4 da Neurons Undergo Dendrite Reshaping

Previous studies indicate that Mmp2 is widely expressed in a variety of tissues, including the PNS and epithelial cells (Page-McCaw et al., 2003). Thus, Mmp2 could be synthesized by either the C4 da neurons or by the surrounding cells. To identify the source of Mmp2 activity, we examined the *Mmp2* expression pattern during early adult stages by using a Gal4 enhancer trap

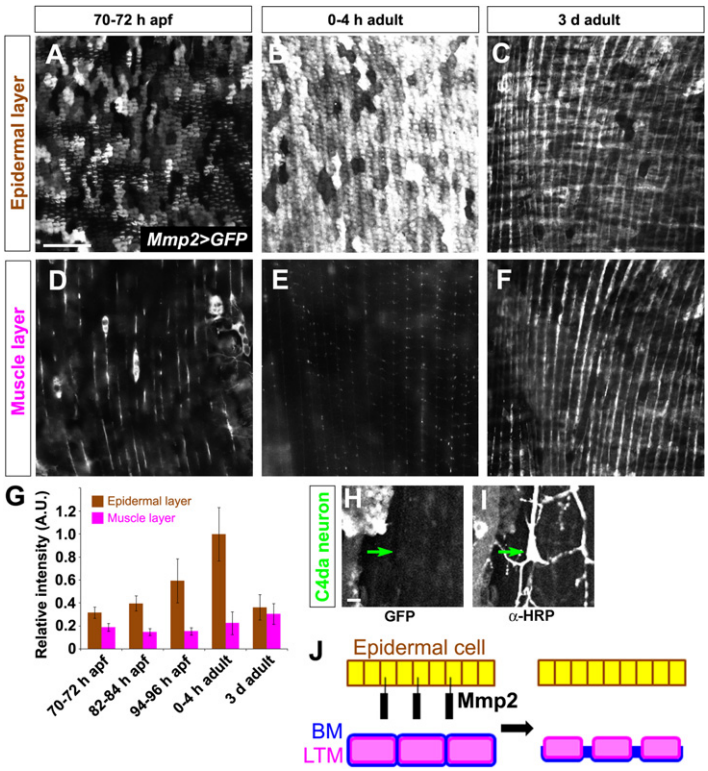

Figure 5. Mmp2 Expression Is Transiently Elevated in Adult Epithelial Cells

(A–C) *Mmp2* expression in epithelial cells is visualized by the *Mmp2-Gal4* driving GFP. Representative images in late pupae (72 hr APF) (A), 0–4 hr adults (B), and 3 day adults (C) are shown.

(D–F) *Mmp2* expression in LTMs is visualized by the *Mmp2*-Gal4 driving GFP. Note that (D), (E), and (F) correspond to the muscle layers underlying the epidermis layer shown in (A), (B), and (C), respectively. The DV-oriented signals between LTM fibers are autofluorescence, because the signals are visible even in animals without the GFP reporter.

(G) Quantification of *Mmp2* expression in epidermal layers and the LTM layers. The values from different images were normalized such that the average GFP intensity of in epidermal layer at the 0–4 hr adult stage (Figure 5B) was defined as 1, and the relative intensity of GFP signals in each time point is showed in the graph (n = 10).

(H and I) In 0–4 hr adults, *Mmp2*-Gal4 driving GFP signal (G) was not detectable in C4 da neurons (H) visualized by anti-HRP staining. Arrows indicate the soma of C4 da neurons.

(J) Schematic representations illustrating the working model of the epithelial Mmp2 in the BM modification. The GPI-anchored proteinase Mmp2 (black) is transiently expressed in epithelial cells (yellow) within 24 hr after eclosion. This epithelial Mmp2 is responsible for the local degradation of the BM (blue) at the interface between the epidermis and the LTMs (magenta). Scale bars, 50 μm.

in *Mmp2* that has been shown to mimic the expression pattern of *Mmp2* to drive expression of GFP (Hayashi et al., 2002; Srivastava et al., 2007). At late pupal stages, we detected only weak GFP expression in epithelial cells (Figure 5A). However, the GFP expression in the epithelial cells was significantly elevated at the early adult stage (0–4 hr after eclosion), precisely at the time at which we observed the BM modification (Figures 5B and 5G). The GFP signal then returned to the basal level by 3 days after eclosion (Figures 5C and 5G). In contrast, we detected very little, if any, GFP expression in the same adult muscle cells (Figures 5D–5G) and sensory neurons (Figures 5H and 5I) during early adult stages. These observations suggest that Mmp2 expression is transiently upregulated in the epithelial cells during 24 hr after eclosion, which presumably triggers the BM modification (Figure 5J).

Mmp2 in Epithelial Cells Drives Dendrite Reshaping through BM Modification

Given that Mmp2 is a GPI-anchored protein (Llano et al., 2002), we reasoned that the epithelial expression of Mmp2 might cause the local degradation of the BM at the interface between the epidermis and the LTMs. To examine this possibility, we generated epithelial clones that were deficient in *Mmp2* functions by using a system in which clones of mutant cells are readily identified by the absence of nuclear RFP (Figure 6A; see Experimental Procedures for detailed information). Our heat-shock protocol efficiently produced large clusters of epithelial clones (20–30 cells), but no muscle clones in the LTMs (Figures 6B–6D; Figure S3). Through the use of this clonal system, we monitored the VKG::GFP expression (as a marker for the BM) over *Mmp2* mutant epithelial clones and found that the VKG::GFP signals underneath the $Mmp2^{-/-}$ homozygous mutant clones accumulated at levels much higher than underneath the $Mmp2^{-/+}$ heterozygous cells outside of the clone (Figure 6D; Figure S3), demonstrating that Mmp2 is required for the BM modification. In contrast, no obvious defect in the BM modification was observed over the epithelial *Mmp1*clones (Figure 6C; Figure S3), one of the two Mmps in *Drosophila* (Page-McCaw et al., 2007). In addition, the BM degradation defects underneath *Mmp2* clones were not rescued by Mmp1 expression (Figure S4). These results suggest that Mmp2, but not Mmp1, is required in the epithelial cells to ensure the proper BM modifications that occur in young adults shortly after eclosion.

We next assessed the role of Mmp2-mediated BM modification in the C4 da dendrite reshaping by comparing the dendrite patterning over the *Mmp2* mutant clones (Figures 7D–7F) to that over the wild-type clones (Figures 7A–7C). C4 da dendrites grow extensively over wild-type and *Mmp2* epithelial cells, with multiple dendrite branches often coursing over epithelial cells, suggesting that the BM modification is not required for dendrite growth and branching. However, although the gross morphology of dendrites was not obviously affected in *Mmp2* mutant clones, the number of terminal branches oriented along the LTM fibers was significantly reduced underneath the *Mmp2* epithelial clones compared with wild-type controls (Figures 7D–7F). In wild-type epithelial clones, over 50% (55.5 ± 3.0%; n = 5) of the dendritic branches were aligned with LTMs both inside and outside of clones in the 2 day adults (Figure 7G). In comparison, only ~30% (27.1 ± 3.6%; n = 7) of the total branches were aligned to the LTMs inside of the Mmp2 clones, whereas ~50% (46.1 ± 4.0%; n = 7) of the total branches were aligned outside of the clones (Figure 7G). A similar reduction in the

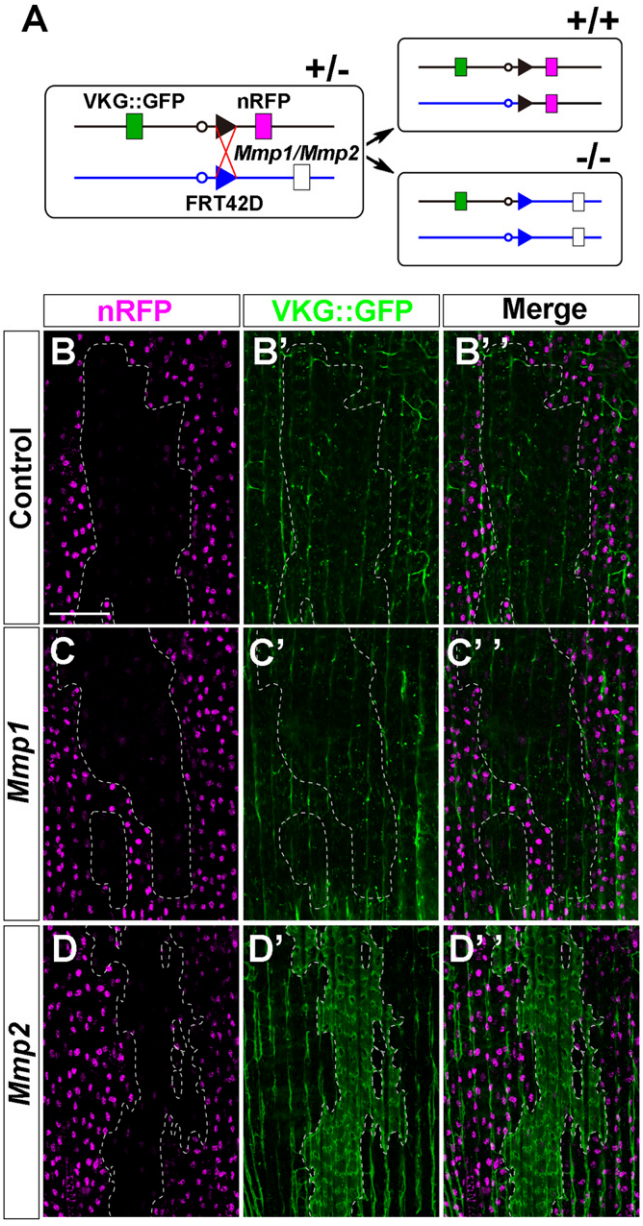

Figure 6. Mmp2, but Not Mmp1, in Epithelial Cells Is Required for Modification of BM upon which C4 da Neurons Innervate

(A) Schematic representation showing the system used to analyze the BM (VKG::GFP) dynamics underneath the *Mmp1* and *Mmp2* null mutant clones (−/−) that are marked by the loss of nucleus RFP (magenta).

(B–C) Mosaic clones for wild-type control (B–B''), *Mmp1* (C–C''), and *Mmp2* (D–D'') were generated in the epithelial cells. Clones (boundaries are marked by dotted lines) were identified by the absence of nuclear RFP (magenta) in the epithelial cells (B, C, and D). The BM underlying the epidermis is visualized by VKG::GFP (B', C', and D'). Right panels are the merged images (B,'' C'', and D''). Note that VKG::GFP remained extensively underneath the *Mmp2* epithelial clones (D–D''), but not underneath wild-type control (B–B'') or *Mmp1* epithelial clones (C–C''). No muscle clones were detectable under the heat-shock conditions that we used to make the epithelial clones (Figure S2). Scale bar, 50 μm. Clone genotypes: *yw, hsFLP; VKG::GFP, FRT42D* (B–B''); *yw, hsFLP; VKG::GFP, FRT42D, Mmp1*^{2} (C–C''); and *yw, hsFLP; VKG::GFP, FRT42D, Mmp2*$^{l(2)k07511}$ (D–D''). We examined 6 of the wild-type clones, 16 of *Mmp1* clones, and 19 of *Mmp2* clones. Multiple clones of each genotype are shown in Figure S4.

aligned terminal number was observed inside of *Mmp2* clones, but not in wild-type clones (Figure 7H). These data are consistent with the model in which the dendrite reshaping requires the epithelial Mmp2-dependent local modification of the BM on which C4 da dendrites grow (Figure 7I).

DISCUSSION

Large-scale reshaping of dendritic arbors is observed in the CNS and PNS including RGCs, olfactory neurons, and cortical neurons (Cline, 2001; Hickmott and Steen, 2005; Wong and Ghosh, 2002). In all cases, the dendrite reshaping is thought to be achieved mostly by elimination of existing dendrite branches and/or growth of new dendrite branches, although detailed analysis of these reshaping events has been hampered by the difficulty in visualizing the entire dendrite arbor of throughout the reshaping process. In this report, we show that large-scale reshaping of the entire dendrite arbor occurs in adult *Drosophila* sensory neurons over a 24 hr period following eclosion (Figure 1). Surprisingly, this dendrite reshaping is achieved by the rearrangement of the existing branches, rather than by extensive pruning of the existing dendrites and elongation of new branches. Indeed, our time-lapse imaging indicates that major branches were rearranged, moving laterally toward the groove between the LTM fibers just after eclosion (Figure 2H). This dendrite rearrangement requires the activity of the Mmp2, as the rearrangement is completely blocked in *Mmp2* mutants (Figure 3). Further genetic analyses indicate that the Mmp2-mediated degradation of the BM drives the dendrite rearrangement (Figures 6 and 7). Finally, Mmp2 expression is upregulated at the precise location (epithelial cells) and time (just following eclosion) at which it is required for this dendrite rearrangement (Figure 5), suggesting that the precise spatiotemporal regulation of Mmp2 expression is one mechanism to achieve this large-scale dendrite arbor reshaping.

In addition to the rearrangement of existing dendrite branches, we found that *Mmp2* also regulates elongation of terminal branches along the DV axis (Figure 2I). Notably, our time-lapse imaging indicates that nascent protrusions often sprouted both inside and outside of the grooves; however, the latter ones immediately disappeared, suggesting that new protrusions sprouting inside of the grooves are selectively maintained (Figure 2I). In addition, although some growing terminals extended toward the outside of the grooves, they immediately retracted back to the groove, and then restarted elongation inside the grooves (Figure 2I). These branch growth behaviors suggest that the terminal elongation is promoted by the microenvironment inside the grooves and/or inhibited by the microenvironment outside the grooves. Most likely, Mmp2-mediated modification of the ECM provides such a microenvironment, since the DV-directed elongation of terminal branches was inhibited in *Mmp2* mutants (Figure 3M).

Mammalian MMPs have been implicated in the structural plasticity of spines (Meighan et al., 2006; Wang et al., 2008; Wilczynski et al., 2008) and dendrites (Gonthier et al., 2009; Szklarczyk et al., 2002); however, the existence of more than 20 MMPs in mammals constrains genetic dissection of in vivo functions. In contrast, *Drosophila* has only two MMPs, Mmp1 and Mmp2, thus providing opportunity to analyze the neural functions of

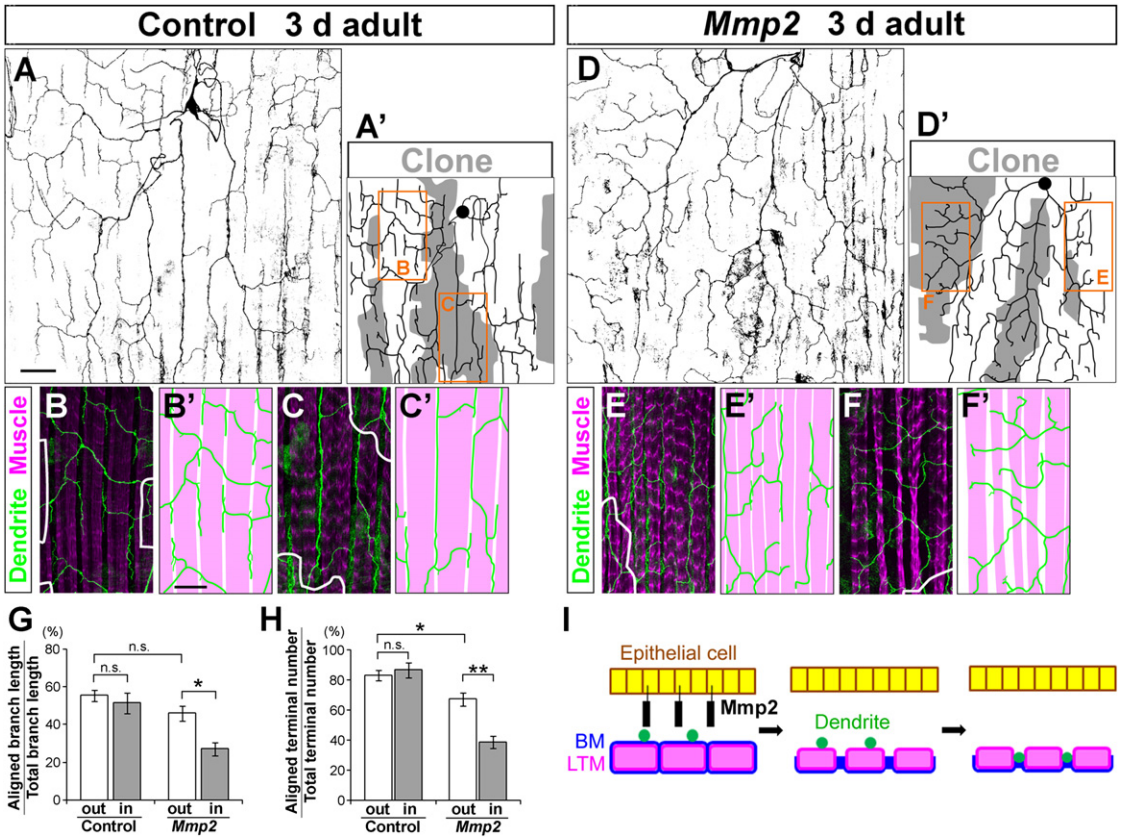

Figure 7. Mmp2-Mediated BM Degradation Triggers Dendrite Reshaping

(A–F) Morphology of C4 da dendrites in the region directly below the epidermal clones was monitored for wild-type control (A–C') or *Mmp2* mutant epithelial clones (D–F'). (A') and (D') are tracings of dendrites in (A) and (D), respectively. The regions covered by the epithelial clones are gray. (B) and (E) are representative images of dendrites (green) and LTMs (magenta) outside the clones, whereas (C) and (F) are directly underneath the clones. White lines mark outlines of clones. Clone genotypes: *hsFLP, ppkGal4, UAS-mCD8GFP; FRT42D* (A) and *hsFLP, ppkGal4, UAS-mCD8GFP; FRT42D, Mmp2$^{l(2)k07511}$* (D).

(G and H) Quantification of the aligned branch length normalized to the total branch length (G) and the aligned terminal number normalized to the total terminal number (H) outside (out, white bars) and underneath (in, gray bars) clones. Error bars indicate the mean ± SEM (wild-type control, n = 5; *Mmp2*, n = 7). *$p < 0.05$, **$p < 0.01$. n.s., not significant ($p > 0.05$) (Student's t test).

(I) Schematic representations showing the model in which Mmp2-mediated BM degradation drives the dendrite reshaping. Epithelial cells, yellow; Mmp2, black; BM, blue; LTMs, magenta; and C4 da dendrites, green. Scale bars, 50 μm (A and D) and 20 μm (B–C' and E–F').

MMPs (Llano et al., 2000, 2002; Page-McCaw et al., 2003). In this study we have provided genetic evidence that Mmp2 is essential for dendrite reshaping through modification of the BM upon which the C4 da dendrites innervate. The mammalian MMPs are known to cleave multiple ECM components, including laminins and collagens (Page-McCaw et al., 2007). Although less information is available for the substrate of the *Drosophila* Mmps, several biochemical studies suggest that Mmp1 and Mmp2 are able to cleave multiple ECM components in vitro as well (Llano et al., 2000, 2002). Indeed, Mmp1 and Mmp2 are both involved in the BM degradation in imaginal disc eversion and in epithelial tumor invasion in vivo (Srivastava et al., 2007; Uhlirova and Bohmann, 2006). However, despite their shared roles in many systems, Mmp2, but not Mmp1, is required for the BM degradation during dendrite reshaping (Figure 6). This specific function of Mmp2 in the dendrite reshaping presumably arises from the transient upregulation of Mmp2 in the epithelial cells during 0–24 hr after eclosion (Figure 5). In addition, Mmp2 is a GPI-anchored protein, whereas Mmp1 is a secreted proteinase, suggesting that the epithelial-derived Mmp2 is likely tethered to the epithelial cell surface (Figure 5J). It is thus possible that the localized Mmp2 activity ensures the local degradation of the BM at the interface between the epidermis and the LTMs (Figure 7I). Collectively, the spatiotemporally regulated expression of Mmp2 provides one molecular explanation for how the BM upon which C4 da dendrites grow is modulated in a specific pattern during the particular time window.

We propose that the Mmp2-mediated BM degradation drives the dendrite reshaping in adult C4 da neurons. This idea is supported by the following lines of evidence. First, the reshaping dendrites are in direct contact with the BM, as revealed by EM experiments (Figure 4). Second, Mmp2 expression is transiently elevated in the epithelial cells at the exact time that C4 da neurons undergo dendrite reshaping (Figure 5). Third, Mmp2 acts locally, since *Mmp2* mutant epithelial clones affect the dendrite reshaping only in dendrites situated directly below the *Mmp2* mutant epithelial cells (Figure 7). Lastly, dendrite reshaping, but not dendrite growth/branching, is completely blocked in *Mmp2* mutants

(Figure 3). How does the BM degradation promote the dendrite reshaping? One possible scenario is that Mmp2 may loosen the dendrite-BM interaction, thereby facilitating the branch dynamics. The remnant BM might also function as a "template" for the dendrite reshaping, since the reshaped branches appeared to be in contact with the remnant BM in the grooves between the LTMs (Figures 4E and 4E'). In regard to this possibility, it is notable that the ECM plays a critical role for dendrite morphogenesis through the direct interaction with the cell adhesion molecules, such as integrins (Reichardt and Tomaselli, 1991). It is thus feasible that the dynamic changes of the ECM distribution upon which C4 da neurons grow may impact the dendrite patterning. In support of this model, the reshaped dendrites extended new terminals (Figure 2I). Alternatively, Mmp2 might release molecules required for the dendrite reshaping from bound stores. Recent reports demonstrate that several axon guidance molecules, such as Semaphorins, Netrin, and Robos, also function as guidance factors for dendrites. For example, Semaphorin 3A acts as an attractive signal for the apical dendrites of pyramidal neurons in the mouse cortex (Polleux et al., 2000). Similarly, dendrites of motoneurons in *Drosophila* CNS are attracted by Netrin and/or Slit (Furrer et al., 2003). Since the secreted guidance molecules are often associated with the ECM, it is possible that the Mmp2-mediated BM degradation may cause a redistribution of the dendrite guidance factors on the ECM, thereby leading to reshaping of dendritic patterns. Finally, it is also possible that Mmp2 modulates the activity of important molecules for the dendrite reshaping by direct cleavage.

MMP expression levels are elevated in a number of neuronal pathologies and after nervous system injury. For example, MMP9 expression is elevated shortly after ischemia (Yong et al., 2001). Likewise, multiple MMPs are immediately induced within 24 hr of an acute insult, such as spinal cord compression injury (Wells, et al., 2003). Interestingly, increased dendrite dynamics have been observed in animal models of pathological conditions, such as the dentate gyrus following temporal lobe epilepsy and in CA1 hippocampal neurons following global ischemia (Spigelman et al., 1998, Ruan et al., 2006). It is thus possible that upregulation of MMPs might contribute to the deregulation of dendrite dynamics under these pathological conditions. In the context of neuronal development, extensive dendrite reshaping occurs in the central and peripheral nervous systems during the critical period, and the reshaping is likely induced by afferent activity (Cline, 2001; Wong and Ghosh, 2002). Although intrinsic factors, including calcium signaling, have been implicated in this dendrite reshaping, the role of ECM dynamics in the critical period remains largely unknown. Recent studies indicate that MMP9 is significantly induced in the hippocampus and the cortex by elevated neural activity (Szklarczyk et al., 2002; von Gertten et al., 2003). Therefore, it would be of great interest to examine whether regulated proteolysis of the local ECM by MMPs might be a conserved mechanism to drive the reshaping of dendrite arbors in both developmental and pathological conditions.

EXPERIMENTAL PROCEDURES

Fly Strains

Fly strains used were: *ppkGal4* (Kuo et al., 2005); *UAS-mCD8GFP*, *VKG::GFP* (Morin et al., 2001); $Mmp1^{2}$ (null allele [Page-McCaw et al., 2003]); $Mmp2^{l(2)k07511}$ (null allele [Page-McCaw et al., 2003]); $Mmp2^{F219I}$ (hypomorphic allele [Page-McCaw et al., 2003]); *Df(2R)Uba1-Mmp2* (Page-McCaw et al., 2003); *Mmp2Gal4* (NP0509, DGRC); and *UAS-GFPT2*. For live imaging of the LTM fibers, the transgenic line expressing mCherry under the MHC promoter was generated by inserting the MHC promoter sequence (Hess et al., 2007) and mCherry ORF into EcoRI and XbaI of pCasper followed by standard P element-mediated transformation. For the clonal analysis, the Histone 2A-mRFP insertion at 44B2 (Bloomington no. 23651) was recombined with the *FRT42D* chromosome, followed by recombination with the *VKG::GFP* chromosome.

Immunohistochemistry

Abdominal cuticles were dissected and fixed in 4% paraformaldehyde in PBS for 30–60 min at room temperature, followed by blocking for 30 min in PBS containing 0.3% Triton X-100 and 5% normal goat serum. Tissues were stained with rat anti-mCD8 (1:200; Caltag) and/or mouse anti-armadillo (DSHB; N2 7A1, 1:15). Primary antibodies were detected with Cy2-conjugated goat anti-rat or Cy5-conjugated goat anti-mouse secondary antibodies (Jackson Research). LTM fibers were labeled with phalloidin-TRITC (1:200; Sigma) or Alexa647-phalloidin (1:200; Invitrogen). Images were taken on a Leica TCS SP5 confocal microscope (Leica). As an alternative to antibody staining, we imaged GFP and mCherry fluorescence in living animals by mounting them in silicon oil (Shin-Etsu). Maximum projections of z-stacks were used in all cases. Images were adjusted for brightness and contrast with Adobe Photoshop (Adobe Systems, San Jose, CA).

Time-Lapse Imaging

Adult flies with *ppkGal4, UAS-mCD8GFP*, and *MHC::mCherry* were etherized and their legs were removed. The wings were fixed on a glass slide with double-stick tape, and the flies were mounted in silicon oil on a cover slip. A wall of silicon grease was built around the flies to maintain high humidity. Images of z-stacks were taken with the confocal system with an oil immersion objective (40×/1.25–0.75; Leica) every 2 min for 4–12 hr at room temperature. After image acquisition, maximized projections of the image stacks were adjusted for brightness and contrast and then converted into QuickTime movies with ImageJ (NIH, Bethesda, MD).

Quantitative Analysis

For simultaneous visualization of dendrites and muscle fibers, flies with *ppkGal4*, *UAS-mCD8GFP*, and *MHC::mCherry* were used in wild-type control or *Mmp2* mutant background. The 0, 1, 2, and 3 day adult stages correspond to 6, 24, 48, and 72 hr ± 2 hr, respectively. The dendrite length was measured by using ImageJ plug-in, NeuronJ. For the phenotypic and quantitative analyses, we focused on the ventral-lateral C4 da dendrites in A4 and A5 segments (Figure 1A), since A4 and A5 neurons exhibit similar and consistent dendrite branch length and branch points. For the quantification in Figures 2, 3, and 7, we measured the total branch length of the ventral half of the dendritic fields, because the dorsal half partially overlaps with the dendritic fields of other *ppk*-positive neurons in the same segment. The data represent the average of multiple single neurons (the counted cell number is shown in the legend). We confirmed that the dendrite reshaping occurs in both males and females in the same schedules (Figure S1). We also confirmed that the dendrite reshaping defects in *Mmp2* mutants are observed in males and females (Figure S1). All data shown in figures are those taken by using females. We defined the aligned branch as the branch along the grooves between the LTMs, and the aligned terminals as the distal part of the branch along the grooves between the LTMs.

EM

Abdominal cuticles were dissected in Ringer's solution and fixed in 2% paraformaldehyde and 2.5% glutaraldehyde in 0.1 M cacodylic buffer at room temperature for 3 hr, followed by washing twice in 30% sucrose in 0.1 M cacodylic buffer for 5 min on ice. The fixed tissues were kept on ice overnight. The specimens were processed for EM by standard techniques, as described previously (Suzuki and Hirosawa, 1994).

Clonal Analysis

To generate epithelial clones in adult abdomen, *yw, hsFLP; VKG::GFP, FRT42D, His2A-mRFP* were mated with *yw, hsFLP; FRT42D/CyO*, *yw, hsFLP;*

FRT42D, Mmp1^{2}*/CyO,* or *yw hsFLP; FRT42D, Mmp2*$^{l(2)k07511}$*/CyO* flies. Embryos were collected for 1 day and subjected to 37°C heat shock for 1 hr on the fifth and seventh day after egg laying. The pupae were kept at 25°C, and adults were examined for the epithelial clones, which are marked by the loss of nucleus RFP signals. No muscle clones were obtained by using this heat shock protocol.

SUPPLEMENTAL INFORMATION

Supplemental Information includes two movies, one table, and four figures and can be found with this article online at doi:10.1016/j.devcel.2010.02.010.

ACKNOWLEDGMENTS

We gratefully acknowledge Y.N. Jan, A. Page-McCaw, the Bloomington Stock Center, and the Kyoto Stock Center for fly stocks; S.I. Bernstein for the promoter of myosin heavy chain gene; Y. Hiromi, K.-I. Kimura, and D. Yamamoto for helpful suggestions; J.Z. Parrish for critical comments on the manuscript; T. Uemura for communicating data before publishing; and Y. Nagashima for expert technical assistance. This work is supported by Grants-in-Aid for Scientific Research, JSPS (to K.E.).

Received: September 14, 2009
Revised: January 23, 2010
Accepted: February 11, 2010
Published: April 19, 2010

REFERENCES

Bodmer, R., and Jan, Y.N. (1987). Morphological differentiation of the embryonic peripheral neurons in *Drosophila*. Roux's Arch. Dev. Biol. *196*, 69–77.

Bodnarenko, S.R., and Chalupa, L.M. (1993). Stratification of On and Off ganglion cell dendrites is dependent on glutamate-mediated afferent activity in the developing retina. Nature *364*, 144–146.

Cline, H.T. (2001). Dendrite arbor development and synaptogenesis. Curr. Opin. Neurobiol. *11*, 118–126.

Dzwonek, J., Rylski, M., and Kaczmarek, L. (2004). Matrix metalloproteinases and their endogenous inhibitors in neuronal physiology of the adult brain. FEBS Lett. *567*, 129–135.

Emoto, K., He, Y., Ye, B., Grueber, W.B., Adler, P.N., Jan, L.Y., and Jan, Y.N. (2004). Control of dendritic branching and tiling by the Tricornered-Kinase/Furry signaling pathway in *Drosophila* sensory neurons. Cell *119*, 245–256.

Emoto, K., Parrish, J.Z., Jan, L.Y., and Jan, Y.N. (2006). The tumour suppressor Hippo acts with the NDR kinases in dendritic tiling and maintenance. Nature *443*, 210–213.

Frischknecht, R., Heine, M., Perrais, D., Seidenbecher, C.I., Choquet, D., and Gundelfinger, E.D. (2009). Brain extracellular matrix affects AMPA receptor lateral mobility and short-term synaptic plasticity. Nat. Neurosci. *12*, 897–904.

Furrer, M.P., Kim, S., Wolf, B., and Chiba, A. (2003). Robo and Frazzled/DCC mediate dendritic guidance at the CNS midline. Nat. Neurosci. *6*, 223–230.

Gao, F.B. (2007). Molecular and cellular mechanisms of dendritic morphogenesis. Curr. Opin. Neurobiol. *17*, 525–532.

Gao, F.B., Brenman, J.E., Jan, L.Y., and Jan, Y.N. (1999). Genes regulating dendritic outgrowth, branching, and routing in *Drosophila*. Genes Dev. *13*, 2549–2561.

Gonthier, B., Koncina, E., Satkauska, S., Perraut, M., Roussel, G., Aunis, D., Kapfhammer, J.P., and Bagnard, D. (2009). A PKC-dependent recruitment of MMP-2 controls Semaphorin-3A growth-promoting effect in cortical dendrites. PLoS ONE *4*, e5099. 10.1371/journal.pone.0005099.

Grueber, W.B., Jan, L.Y., and Jan, Y.N. (2002). Tiling of the *Drosophila* epidermis by multidendritic sensory neurons. Development *129*, 2867–2878.

Hayashi, S., Ito, K., Sado, Y., Taniguchi, M., Akimoto, A., Takeuchi, H., Aigaki, T., Matsuzaki, F., Nakagoshi, H., Tanimura, T., et al. (2002). GETDB, a database compiling expression patterns and molecular localization of a collection of Gal4 enhancer traps. Genesis *34*, 58–61.

Hess, N.K., Singer, P.A., Trinh, K., Nikkhoy, M., and Bernstein, S.I. (2007). Transcriptional regulation of the *Drosophila melanogaster* muscle myosin heavy-chain gene. Gene Expr. Patterns *7*, 413–422.

Hickmott, P.W., and Steen, P.A. (2005). Large-scale changes in dendritic structure during reorganization of adult somatosensory cortex. Nat. Neurosci. *8*, 140–142.

Holtmaat, A.J., Trachtenberg, J.T., Wilbrecht, L., Shepherd, G.M., Zhang, X., Knott, G.W., and Svoboda, K. (2005). Transient and persistent dendritic spines in the neocortex in vivo. Neuron *45*, 279–291.

Jan, Y.N., and Jan, L.Y. (2003). The control of dendrite development. Neuron *40*, 229–242.

Kimura, K.I., and Truman, J. (1990). Postmetaphorphic cell death in the nervous and muscular systems of *Drosophila melanogaster*. J. Neurosci. *10*, 403–411.

Koike-Kumagai, M., Yasunaga, K., Morikawa, R., Kanamori, T., and Emoto, K. (2009). The target of rapamycin complex 2 (TORC2) controls dendritic tiling of *Drosophila* sensory neurons through the Tricornered kinase signaling pathway. EMBO J. *28*, 3879–3892.

Kuo, C.T., Jan, L.Y., and Jan, Y.N. (2005). Dendrite-specific remodeling of *Drosophila* sensory neurons requires matrix metalloproteases, ubiquitin-proteasome, and ecdysone signaling. Proc. Natl. Acad. Sci. USA *102*, 15230–15235.

Llano, E., Adam, G., Pendas, A.M., Quesada, V., Sanchez, L.M., Santamaria, I., Noselli, S., and Lopez-Otin, C. (2002). Structural and enzymatic characterization of *Drosophila* Dm2-MMP, a membrane-bound matrix metalloproteinase with tissue-specific expression. J. Biol. Chem. *277*, 23321–23329.

Llano, E., Pendas, A.M., Aza-Blanc, P., Kornberg, T.B., and Lopez-Otin, C. (2000). Dm1-MMP, a matrix metalloproteinase from *Drosophila* with a potential role in extracellular matrix remodeling during neural development. J. Biol. Chem. *275*, 35978–35985.

Lohmann, C., and Wong, R.O. (2005). Regulation of dendritic growth and plasticity by local and global calcium dynamics. Cell Calcium *37*, 403–409.

Magata, N., Mizuguchi, Y., and Hensch, T.K. (2004). Experience-dependent pruning of dendritic spines in visual cortex by tissue plasminogen activator. Neuron *44*, 1031–1041.

Malun, D., and Brunjes, P.C. (1996). Development of olfactory glomeruli: temporal and spatial interactions between olfactory receptor axons and mitral cells opossums and rats. J. Comp. Neurol. *368*, 1–16.

Marrs, G.S., Honda, T., Fuller, L., Thangavel, R., Balsamo, J., Lilien, J., Dailey, M.E., and Arregui, C. (2006). Dendritic arbors of developing retina ganglion cells are stabilized by beta 1-integrins. Mol. Cell. Neurosci. *32*, 230–241.

Meighan, S.E., Meighan, P.C., Choudhury, P., Davis, C.J., Olson, M.L., Zornes, P.A., Wright, J.W., and Harding, J.W. (2006). Effects of extracellular matrix degrading proteases matrix metalloproteinase 3 and 9 on spatial learning and synapse plasticity. J. Neurochem. *96*, 1227–1241.

Mizrahi, A. (2007). Dendritic development and plasticity of adult-born neurons in the mouse olfactory bulb. Nat. Neurosci. *10*, 444–452.

Moresco, E.M., Donaldson, S., Williamson, A., and Koleske, A.J. (2005). Integrin-mediated dendrite branch maintenance requires Abelson (Abl) family kinases. J. Neurosci. *25*, 6105–6118.

Morin, X., Daneman, R., Zavortink, M., and Chia, W. (2001). A protein trap strategy to detect GFP-tagged proteins expressed from their endogenous loci in *Drosophila*. Proc. Natl. Acad. Sci. USA *98*, 15050–15055.

Oray, S., Majewska, A., and Sur, M. (2004). Dendritic spine dynamics are regulated by monocular deprivation and extracellular matrix degradation. Neuron *44*, 1021–1030.

Page-McCaw, A., Serano, J., Sante, J.M., and Rubin, G.M. (2003). *Drosophila* matrix metalloproteinases are required for tissue remodeling, but not embryonic development. Dev. Cell *4*, 95–106.

Page-McCaw, A., Ewald, A., and Werb, Z. (2007). Matrix metalloproteinases and the regulation of tissue remodeling. Nat. Rev. Mol. Cell Biol. *8*, 221–233.

Parrish, J.Z., Emoto, K., Kim, M.D., and Jan, Y.N. (2007). Mechanisms that regulate establishment, maintenance, and remodeling of dendritic fields. Annu. Rev. Neurosci. *30*, 399–423.

Pavlov, I., Lauri, S., Taira, T., and Rauvala, H. (2004). The role of ECM molecules in activity-dependent synaptic development and plasticity. Birth Def. Res. C Embryo Today *72*, 12–24.

Polleux, F., Morrow, T., and Ghosh, A. (2000). Semaphorin 3A is a chemoattractant for cortical apical dendrites. Nature *404*, 567–573.

Reichardt, L.F., and Tomaselli, K.J. (1991). Extracellular matrix molecules and their receptors: functions in neural development. Annu. Rev. Neurosci. *14*, 531–570.

Ruan, Y.W., Zou, B., Fan, Y., Li, Y., Li, N., Zheng, Y.S., Gao, T.M., Yao, Z., and Xu, Z.C. (2006). Dendritic plasticity of CA1 pyramidal neurons after transient global ischemia. Neuroscience *140*, 191–201.

Sekine-Aizawa, Y., Hama, E., Watanabe, K., Tsubuki, S., Kanai-Azuma, M., Kanai, Y., Arai, H., Aizawa, H., Iwata, N., and Saido, T.C. (2001). Matrix metalloproteinase (MMP) system in brain: identification and characterization of brain-specific MMP highly expressed in cerebellum. Eur. J. Neurosci. *13*, 935–948.

Shimono, K., Fujimoto, A., Tsuyama, T., Yamamoto-Kochi, M., Sato, M., Hattori, Y., Sugimura, K., Usui, T., Kimura, K., and Uemura, T. (2009). Multidendritic sensory neurons in the adult *Drosophila* abdomen: origin, dendritic morphology, and segment- and age-dependent programmed cell death. Neural Dev. *4*, 37. 10.1186/1749-8104-4-37.

Spigelman, I., Yan, X.X., Obenaus, A., Lee, E.Y., Wasterlain, C.G., and Ribak, C.E. (1998). Dentate granule cells form novel basal dendrites in a rat model of temporal lobe epilepsy. Neuroscience *86*, 109–120.

Srivastava, A., Pastor-Pareja, J.C., Igaki, T., Pagliarini, R., and Xu, T. (2007). Basement membrane remodeling is essential for *Drosophila* disc eversion and tumor invasion. Proc. Natl. Acad. Sci. USA *104*, 2721–2726.

Suzuki, E., and Hirosawa, K. (1994). Immunolocalization of a *Drosophila* phosphatidylinositol transfer protein (rdgB) in normal and *rdg*A mutant photoreceptor cells with special reference to the subrhabdomeric cisternae. J. Electron Microsc. (Tokyo) *43*, 183–189.

Szklarczyk, A., Lapinska, J., Rylski, M., McKay, R.D., and Kaczmarek, L. (2002). Matrix metalloproteinase-9 undergoes expression and activation during dendritic remodeling in adult hippocampus. J. Neurosci. *22*, 920–930.

Uhlirova, M., and Bohmann, D. (2006). JNK- and Fos-regulated Mmp1 expression cooperate with Ras to induce invasive tumor in *Drosophila*. EMBO J. *25*, 5294–5304.

von Gertten, C., Holmin, S., Mathiesen, T., and Nordqvist, A.C. (2003). Increases in matrix metalloproteinase-9 and tissue inhibitor of matrix metalloproteinase-1 mRNA after cerebral contusion and depolarisation. J. Neurosci. Res. *73*, 803–810.

Wang, X.B., Bozdagi, O., Nikiczuk, J.S., Zhai, Z.W., Zhou, Q., and Huntley, G.W. (2008). Extracellular proteolysis by matrix metalloproteinase-9 drives dendritic spine enlargement and long-term potentiation coordinately. Proc. Natl. Acad. Sci. USA *105*, 19520–19525.

Wells, J.E., Hurlbert, R.J., Fehlings, M.G., and Yong, V.W. (2003). Neuroprotection by monocycline facilitates significant recovery from spinal cord injury in mice. Brain *126*, 1628–1637.

Wilczynski, G.M., Konopacki, F.A., Wilczek, E., Lasiecka, Z., Gorlewicz, A., Michaluk, P., Wawrzyniak, M., Malinowska, M., Okulski, P., Kolodziej, et al., (2008). Important role of matrix metalloproteinase 9 in epileptogenesis. J. Cell Biol. *180*, 1021–1035.

Williams, D.W., and Truman, J.W. (2005). Cellular mechanisms of dendrite pruning in *Drosophila*: insights from in vivo time-lapse of remodeling dendritic arborizing sensory neurons. Development *132*, 3631–3642.

Wong, R.O.L., and Ghosh, A. (2002). Activity-dependent regulation of dendritic growth and pattering. Nat. Rev. Neurosci. *3*, 803–812.

Yong, V.W. (2005). Metalloproteinases: mediators of pathology and regeneration in the CNS. Nat. Rev. Neurosci. *6*, 931–944.

Yong, V.W., Power, C., Forsyth, P., and Edwards, D.R. (2001). Metalloproteinases in biology, pathology of the nervous system. Nat. Rev. Neurosci. *2*, 502–511.

Zuo, Y., Lin, A., Chang, P., and Gan, W.B. (2005). Development of long-term dendritic spine stability in diverse regions of cerebral cortex. Neuron *46*, 181–189.